Proceedings of the 2003 IEEE/ASME
International Conference on
Advanced Intelligent Mechatronics (AIM 2003)

Solution of Human-like Redundant Manipulator Mounted on Flexible Body for Task-space Feedback Control

Jun Ueda*, Reishi Oya*, Tsukasa Ogasawara*, and Tsuneo Yoshikawa**
* Graduate School of Information Science,
Nara Institute of Science and Technology (NAIST), Nara, 630-0192, Japan,
E-mail:{uedajun, reishi-o, ogasawar}@is.aist-nara.ac.jp
** Department of Mechanical Engineering, Kyoto University, Kyoto, 606-8501, Japan,
E-mail:yoshi@mech.kyoto-u.ac.jp

Abstract— **In this paper, the concept of the 'robust arm configuration' (RAC) is expanded to the redundancy solution of a redundant manipulator mounted on a flexible body for task-space feedback control. The RAC measure is used to determine the redundant degree of freedom of the manipulator. If the arm configuration is near or on the RAC, a high-gain task-space feedback using Jacobian transpose can be applied without considering the base flexibility, i.e., additional sensor or solution of a whole inverse dynamics are not necessary. It leads to the separation of the manipulator control and the mobile base control without losing the stability. The validity is confirmed by a numerical example performed with a 4 DOF human-like redundant manipulator mounted on a 1 DOF flexible base. The arm angle is determined for a desired tip position based on the RAC measure.**

Keywords— **Flexible Robots, Flexible Base, Mechanical Resonance, Modal Analysis, Task-space Control, Passivity, Redundancy.**

I. Introduction

The difficulties of the control of a manipulator mounted on a flexible base has been firstly pointed out and studied in the field of industrial robots and space robots[1]. This problem can be found in recently studied mobile manipulators and humanoid robots where the base flexibility caused not only by the structure but also by servo control of the body. In order to achieve a task precisely, a task-space feedback control, using the positioning error between the end-effector and the desired position, is more desirable than a joint variable control based on the solution of the inverse kinematics. Although the stability of the end point feedback control for a rigid manipulator is guaranteed[2], its application for flexible manipulator is not straightforward[3]. Many researches have been presented on flexible link and elastic joint robots, with respect to joint trajectory control[4], stability of joint-level control[5][6], and feedforward tracking control[7]. Nenchev et. al.[8] proposed a reaction null-space control for a flexible-structure-mounted manipulator. Jiang et. al.[9] proposed the compensability of flexible robot arms which indicates the possibility of compensation of the tip errors due to the link flexibility by the joint displacements. Konno et. al.[10] proposed the modal accessibility based on the controllability of the vibration mode. However, these methods are not directly related to the closed loop performance. Therefore, the task-space control with a flexible base still remains as a difficult problem.

In the meanwhile, many manipulators including human's arm have redundant degree of freedom (DOF). The researches on the determination of this redundancy have long been studied. Yoshikawa[11] proposed the concept of manipulability and many related studies has been presented. However, the manipulability is an open loop measure of a certain arm configuration, therefore, it cannot be used to predict the closed loop performance of flexible mechanisms.

We have shown that a manipulator mounted on a flexible base has the 'robust arm configuration'(RAC)[12], in which the linearized system around the desired tip position is positive real (passive). On or in the neighbor of the RAC, a high-gain task-space feedback using Jacobian transpose can be applied without considering the base flexibility, i.e., additional sensor or solution of a whole inverse dynamics are not necessary. We have also proposed the mode shape compensator[13] which improves the robustness of the configuration using an acceleration feedback.

In this paper, a human-like redundant manipulator is considered which is based on a flexible body such as a mobile base or a walking machine. A redundancy solution of manipulator is proposed based on the RAC measure for precise task-space feedback control. The optimal configuration can be determined which is directly related to a high-bandwidth closed loop control. It leads to the separation[14] of the manipulator control and the mobile base control without losing the stability. The validity of the proposed method is confirmed by a numerical example performed with a 4 DOF Human-like redundant manipulator mounted on a 1 DOF flexible body.

II. Dynamic Model and Problem Statement

A. Flexibility of the Base

A typical situation we are going to study is given in Fig. 1. A 4 DOF human-like redundant manipulator is mounted on a 1 DOF flexible base. The manipulator is attached to the endpoint of the base. The base has flexibility since it is supported by a passive visco-elastic joint θ_1. Considering the structure of a human body, the base corresponds to the shoulder, and the a passive visco-elastic joint, which rotates around z axis, corresponds to the twisting motion of the waist.

In this paper, the tip positioning control to a fixed desired position and its closed loop feedback stability are considered. A continuous feedfoward tracking control including wide range of motion is not considered.

Since the rotation of the tip is not considered, the manipulator has 1 DOF redundancy. Each active joint, θ_2 to θ_5, has an actuator and an encoder. In general, it is difficult to directly measure the deformation of this flexibility. Therefore, we assume that no encoder is attached to this passive joint. The positioning error between the tip and the fixed desired position is directly detected by a camera or other position-detecting sensor attached on the tip. A task-space control (direct visual feedback) is applied using detected positioning error and the Jacobian transpose.

As described above, we assumed that no sensor is attached to the base for measuring the deformation caused by the flexibility. Therefore, if the servo gain of the task-space controller is increased, spillover occurs and the control bandwidth is limited.

Due to the redundant DOF, the manipulator shown in Fig. 1 can choose any elbow position that realizes a given tip position. Kreutz-Delgado et. al. defined the arm angle[15] for a similar manipulator. If the arm angle is changed using the redundancy, the whole dynamics changes accordingly. The main idea of this paper is determination of this redundant DOF to avoid the instability caused by the base flexibility. As a result, a high-gain task-space feedback using Jacobian transpose can be applied without considering the base flexibility, i.e., additional sensor or solution of a whole inverse dynamics are not necessary. It leads to the separation[14] of the manipulator control and the mobile base control without losing the stability of tip positioning.

B. Dynamic Equation and Linearized Model

A general system of an m DOF flexible base supported by m passive visco-elastic elements and an n DOF redundant manipulator is considered, which includes the system of Fig. 1 as a special case. The dynamic equation of the manipulator is assumed to be given by:

$$\boldsymbol{\tau} = \boldsymbol{M}(\boldsymbol{q})\ddot{\boldsymbol{q}} + \boldsymbol{h}(\boldsymbol{q}, \dot{\boldsymbol{q}}) + \boldsymbol{g}(\boldsymbol{q}) \qquad (1)$$

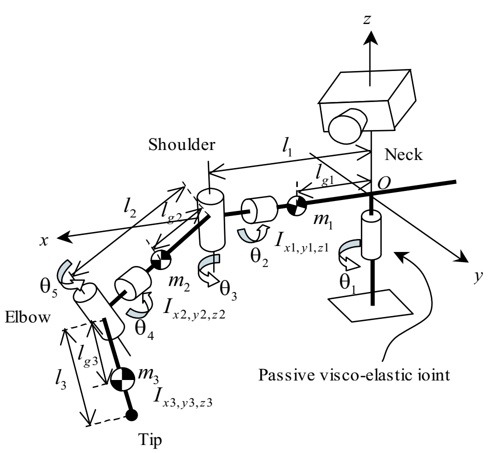

Fig. 1. 4 DOF Redundant Manipulator with 1 DOF Flexible Body

where $\boldsymbol{\tau}$ denotes the joint torque, and $\boldsymbol{q}$ is the joint axis displacement vector. Further, we assume that $\boldsymbol{\tau} = \mathrm{col}[\boldsymbol{\tau}_p, \boldsymbol{\tau}_a] \in \Re^N$ $(N = m + n)$ (column vector is obtained by putting $\boldsymbol{\tau}_p$ and $\boldsymbol{\tau}_a$ in one column) where $\boldsymbol{\tau}_p = [\ \tau_1 \ \ \ldots \ \ \tau_m\ ]^T$ is torque generated by passive visco-elastic joints, and $\boldsymbol{\tau}_a = [\ \tau_{m+1} \ \ \ldots \ \ \tau_{m+n}\ ]^T$ is actuator torque generated by motors. Similarly, we assume that $\boldsymbol{q} = \mathrm{col}[\boldsymbol{q}_p, \boldsymbol{q}_a] \in \Re^N$ where $\boldsymbol{q}_p = [\ \theta_1 \ \ \ldots \ \ \theta_m\ ]^T$ and $\boldsymbol{q}_a = [\ \theta_{m+1} \ \ \ldots \ \ \theta_{m+n}\ ]^T$. The subscript p denotes the passive visco-elastic joints and a denotes the active joints. Note that $\boldsymbol{q}_p$ cannot be measured directly. $\boldsymbol{M}(\boldsymbol{q}) \in \Re^{N\times N}$ denotes the inertia matrix, $\boldsymbol{h}(\boldsymbol{q}, \dot{\boldsymbol{q}})$ is the centrifugal and Coriolis forces, and $\boldsymbol{g}(\boldsymbol{q})$ is the gravity force. The feedback control of the positioning error is necessary to compensate the uncertainty of the inverse kinematics of the manipulator. Uncertainty comes from modeling error of the manipulator and uncertain position of the desired position. Let $\boldsymbol{r} = \boldsymbol{r}(\boldsymbol{q}) \in \Re^n$ be the position of the end effector, $\boldsymbol{r}_d$ be the desired position of $\boldsymbol{r}$, and $\bar{\boldsymbol{q}}_p = [\bar{\theta}_1 \cdots \bar{\theta}_m]^T$ be the equilibrium points of $\boldsymbol{q}_p$. $\boldsymbol{r}_d$ is realized by $\boldsymbol{q}_d = \mathrm{col}[\bar{\boldsymbol{q}}_p, \boldsymbol{q}_{ad}]$ where $\bar{\boldsymbol{q}}_{ad} = [\theta_{(m+1)d} \ \cdots \ \theta_{(m+n)d}]^T$, i.e., $\boldsymbol{r}_d = \boldsymbol{r}(\boldsymbol{q}_d)$. Let $\boldsymbol{r}_v = \boldsymbol{r}_v(\boldsymbol{q}_a)$ be the position of the end effector when the displacement of the base is zero, so that $\boldsymbol{r}(\boldsymbol{q}_d) = \boldsymbol{r}_v(\boldsymbol{q}_{ad})$. It is assumed that the torque $\tau_1, \cdots, \tau_m$ generated by passive joints are given by:

$$\tau_i = k_{pi}(\bar{\theta}_i - \theta_i) - k_{vi}\dot{\theta}_i (i = 1, \cdots, m) \qquad (2)$$

where k_{pi} and k_{vi} are the stiffness and the viscous coefficient respectively, and $\bar{\theta}_1, \cdots, \bar{\theta}_m$ are the equilibrium positions.

Hereafter, the linearized model around $\boldsymbol{r}_d$, (around $\bar{\boldsymbol{q}}_p$, $\boldsymbol{q}_{ad}$ for the joint space) is examined. We assume that the effect of the gravity is compensated beforehand:

$$\boldsymbol{\tau}_a = \tilde{\boldsymbol{\tau}}_a + \boldsymbol{g}(\boldsymbol{q}_a) \qquad (3)$$

$\tilde{\boldsymbol{\tau}}_a$ is a new control input for a feedback control. The centrifugal and Coriolis factor are ignored, since these second-order terms are not related to the closed loop stability based on the linearized model.

Substituting (2) and (3) into (1), we obtain

$$\begin{bmatrix} \boldsymbol{0} \\ \tilde{\boldsymbol{\tau}}_a \end{bmatrix} = \boldsymbol{M}\ddot{\boldsymbol{q}} + \boldsymbol{D}\dot{\boldsymbol{q}} + \boldsymbol{K}(\boldsymbol{q} - \boldsymbol{q}_d) \qquad (4)$$

where $\boldsymbol{D} = \mathrm{diag}\,(k_{v1}, \cdots, k_{vm}, 0, \cdots, 0)$, and $\boldsymbol{K} = \mathrm{diag}\,(k_{p1}, \cdots, k_{pm}, 0, \cdots, 0)$ are the stiffness and the viscous matrix, respectively.

We have assumed that $\boldsymbol{q}_p$, the deformation of the flexibility, cannot be measured. A control law without knowing $\boldsymbol{q}_p$ is given by:

$$\tilde{\boldsymbol{\tau}}_a = \boldsymbol{J}_v^T \boldsymbol{f} \qquad (5)$$

where $\boldsymbol{J}_v = \partial \boldsymbol{r}_v / \partial \boldsymbol{q}_a^T \in \Re^{n\times n}$, and $\boldsymbol{f}$ denotes the control input force calculated by a task-space feedback controller $\boldsymbol{K}_c(s)$. Note that if the mechanism is rigid, this is the most standard task-space controller. Although $\boldsymbol{f}$ is needed to stabilize at least a rigid manipulator, the structure of the feedback controller is not specified at the moment.

Denoting $\boldsymbol{x} = \mathrm{col}\,[\dot{\boldsymbol{q}}, (\boldsymbol{q} - \boldsymbol{q}_d)]$ and $\boldsymbol{y} = \boldsymbol{r}(\boldsymbol{q}) - \boldsymbol{r}(\boldsymbol{q}_d)$, an n-inputs n-outputs state space representation in the task-space is obtained.

$$\dot{\boldsymbol{x}} = \boldsymbol{A}\boldsymbol{x} + \boldsymbol{B}\boldsymbol{f} \tag{6}$$

$$\boldsymbol{y} = \boldsymbol{C}\boldsymbol{x} \tag{7}$$

$$\boldsymbol{A} = \begin{bmatrix} -\boldsymbol{M}^{-1}\boldsymbol{D} & -\boldsymbol{M}^{-1}\boldsymbol{K} \\ \boldsymbol{I} & \boldsymbol{O} \end{bmatrix} \tag{8}$$

$$\boldsymbol{B} = \begin{bmatrix} \boldsymbol{M}^{-1} \begin{bmatrix} \boldsymbol{O}^{m\times n} \\ \boldsymbol{I}^{n\times n} \end{bmatrix} \\ \boldsymbol{O}^{(m+n)\times n} \end{bmatrix} \boldsymbol{J}_v^T \tag{9}$$

$$\boldsymbol{C} = \begin{bmatrix} \boldsymbol{O} & \boldsymbol{J} \end{bmatrix} \tag{10}$$

where $\boldsymbol{J} = \partial \boldsymbol{r}/\partial \boldsymbol{q}^T \in \Re^{n\times(m+n)}$ is a real Jacobian matrix, and $\boldsymbol{O}$ is the matrix whose elements are all zero.

The closed loop system is shown in Fig. 2. The $n \times n$ transfer matrix of the system from $\boldsymbol{f}$ to $\boldsymbol{y}$ is obtained by

$$\boldsymbol{P}(s, \boldsymbol{q}_d) = \boldsymbol{C}(s\boldsymbol{I} - \boldsymbol{A})^{-1}\boldsymbol{B} \tag{11}$$

We use $\boldsymbol{P}(s, \boldsymbol{q}_d)$ when we emphasize that $\boldsymbol{P}(s)$ is a function of $\boldsymbol{q}_d$, otherwise we use $\boldsymbol{P}(s)$. Note that $\boldsymbol{P}(s)$ does not include the feedback controller, but only $\boldsymbol{J}_v^T$. Hence the following analysis is not limited to any specific controller.

C. Modal Analysis

By modal analysis, $\boldsymbol{P}(s)$ can be expressed as a linear sum of a rigid mode and m vibration modes. $\boldsymbol{A}$ has in total $2(n + m)$ poles, $2n$ of these poles are zero, corresponding to the rigid mode, the remaining $2m$ poles are conjugate complex poles corresponding to the vibration modes.

Let $\lambda_0(= 0)$, λ_i, $\bar{\lambda}_i$ ($i = 1, \cdots, m$; $\bar{\lambda}_i$ denotes the complex conjugate of λ_i) be $2m + 1$ distinct eigenvalues of $\boldsymbol{A}$. Here, λ_0 corresponds to the rigid mode, and λ_i and $\bar{\lambda}_i$ correspond to the ith vibration modes, respectively. Using $\boldsymbol{u}_i$ which satisfy: $\boldsymbol{A}\boldsymbol{u}_{2j-1} = \lambda_0\boldsymbol{u}_{2j-1} = \boldsymbol{o}(j = 1, \cdots, n)$, $\boldsymbol{A}\boldsymbol{u}_{2j} = \boldsymbol{u}_{2j-1}$, $\boldsymbol{A}\boldsymbol{u}_{2(n+i)-1} = \lambda_i\boldsymbol{u}_{2(n+i)-1}(i = 1, \cdots, m)$, $\boldsymbol{A}\boldsymbol{u}_{2(n+i)} = \bar{\lambda}_i\boldsymbol{u}_{2(n+i)}$. We define matrix $\boldsymbol{U}$ and $\boldsymbol{V}$ as follows:

$$\boldsymbol{U} \stackrel{\triangle}{=} \begin{bmatrix} \boldsymbol{u}_1 & \cdots & \boldsymbol{u}_{2n} & \boldsymbol{u}_{2n+1} & \cdots & \boldsymbol{u}_{2(m+n)} \end{bmatrix} \tag{12}$$

$$\boldsymbol{V}^* \stackrel{\triangle}{=} \mathrm{col}\left[\boldsymbol{v}_1^*, \boldsymbol{v}_2^*, \cdots, \boldsymbol{v}_{2(m+n)}^*\right] = \boldsymbol{U}^{-1} \tag{13}$$

where $\boldsymbol{v}^*$ denotes the complex conjugate transpose of $\boldsymbol{v}$. Applying $\boldsymbol{U}$ and $\boldsymbol{V}$, a Jordan canonical form of $\boldsymbol{A}$, with n jordan blocks of $\boldsymbol{J}_0$[16], is obtained as:

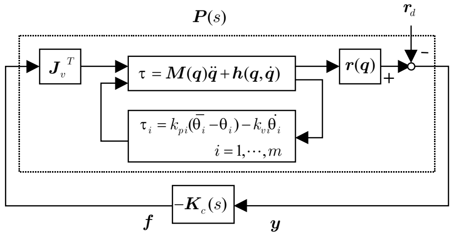

Fig. 2. Task-space Feedback Control

$$\boldsymbol{V}^*\boldsymbol{A}\boldsymbol{U} = \mathrm{diag}(\underbrace{\boldsymbol{J}_0, \cdots, \boldsymbol{J}_0}_{n}, \boldsymbol{\Lambda}) \tag{14}$$

where $\boldsymbol{\Lambda} = \mathrm{diag}(\lambda_1, \bar{\lambda}_1, \cdots, \lambda_{m-1}, \bar{\lambda}_{m-1}, \lambda_m, \bar{\lambda}_m)$ and $\boldsymbol{J}_0 = \begin{bmatrix} 0 & 1 \\ 0 & 0 \end{bmatrix}$. From the partial fraction expansion, the modal analyzed transfer function of $\boldsymbol{P}(s)$ is obtained as:

$$\boldsymbol{P}(s) = \frac{1}{s^2}\boldsymbol{R}_0 + \sum_{i=1}^{m} \frac{1}{s^2 + 2\zeta_i\hat{\omega}_i s + \hat{\omega}_i^2}\boldsymbol{R}_i \tag{15}$$

where

$$\boldsymbol{R}_0 = \sum_{j=1}^{n} \boldsymbol{C}\boldsymbol{u}_{2j-1}\boldsymbol{v}_{2j}^*\boldsymbol{B} = \boldsymbol{J}_v\hat{\boldsymbol{M}}^{-1}\boldsymbol{J}_v^T \tag{16}$$

The matrix $\boldsymbol{R}_0$ corresponds to the rigid body mode and is positive semi-definite. Recall that the linealization has been done around $\bar{\boldsymbol{q}}_p$, we can use $\boldsymbol{J} = [* \ \boldsymbol{J}_v]$. $\hat{\boldsymbol{M}} = [M_{kl}] \in \Re^{n\times n}(m + 1 \le k, l \le m + n)$ is a partial matrix of $\boldsymbol{M}$.

From $\boldsymbol{C}\boldsymbol{B} = \boldsymbol{O}$ and (9), the term of the first order of s vanishes. Hence

$$\boldsymbol{R}_i = -2\mathrm{Re}\left(\bar{\lambda}_i(\boldsymbol{C}\boldsymbol{u}_{2(n+i)-1})(\boldsymbol{v}_{2(n+i)-1}^*\boldsymbol{B})\right) \tag{17}$$

holds. $\boldsymbol{R}_i$ is called the residue matrix. Note that $\boldsymbol{R}_0$ is positive semi-definite and $\mathrm{rank}(\boldsymbol{R}_i) = 1$ at most from (17). In addition, $\hat{\omega}_i = |\lambda_i|$ and $\zeta_i = -\mathrm{Re}(\lambda_i)/|\lambda_i|$ are obtained where ζ_i and $\hat{\omega}_i$ represent the damping coefficient and the natural frequency respectively.

III. Robust Arm Configuration of Manipulator and Robustness Measure

In this section, the robust arm configuration (RAC) of manipulator and its robustness measure are briefly described. For more detail, see[12].

A. Positive Realness of Transfer Function Matrix

The robustness of $\boldsymbol{P}(s, \boldsymbol{q}_d)$ is evaluated based on its positive realness. Let $\boldsymbol{G}(s, \boldsymbol{q}_d)$ be the transfer function from the control input $\boldsymbol{f}$ to the velocity $\dot{\boldsymbol{y}}$:

$$\boldsymbol{G}(s, \boldsymbol{q}_d) \stackrel{\triangle}{=} s\boldsymbol{P}(s, \boldsymbol{q}_d) \tag{18}$$

Similarly, we use $\boldsymbol{G}(\boldsymbol{q}_d, s)$ when we emphasize that $\boldsymbol{G}(s)$ is a function of $\boldsymbol{q}_d$, otherwise we use $\boldsymbol{G}(s)$.

The following theorem concerning the positive realness of the transfer function has been obtained.

Theorem $\boldsymbol{G}(s)$ is positive real if and only if the following conditions 1 and 2 are satisfied for $\forall i : i = 1, \cdots, m, \forall j : j = 1, \cdots, n$

1. $\boldsymbol{R}_i = \boldsymbol{R}_i^T$
2. $\kappa_{jj}^i > 0$ where $\boldsymbol{R}_i = \left[\kappa_{kl}^i\right] \quad (k, l = 1, \cdots, n)$

From the passivity theory, the stability of the system is always guaranteed and no spillover occurs for any velocity feedback if $\boldsymbol{G}(s)$ is positive real[17].

Remark It has been shown that no $\boldsymbol{q}_d$ gives strictly positive real $\boldsymbol{G}(s)$[12]. This fact shows that the dimension of the set of RAC is not equal to that of the workspace.

B. Definition of Robust Arm Configuration

Definition 1 An arm configuration $\boldsymbol{q}_d$ which satisfies

$$\lambda_{min}(\boldsymbol{G}_i(j\omega, \boldsymbol{q}_d) + \boldsymbol{G}_i^T(-j\omega, \boldsymbol{q}_d)) = 0, \forall\omega \in \Re \qquad (19)$$

is called 'robust arm configuration' (RAC) for ith mode where

$$\boldsymbol{G}_i(s) \triangleq \frac{s}{s^2 + 2\zeta_i\hat{\omega}_i s + \hat{\omega}_i^2}\boldsymbol{R}_i \qquad (20)$$

The robust arm configuration is a special configuration for which the linearized system is positive real (passive). The stability of the ith mode is guaranteed for any velocity feedback.

Definition 2 An arm configuration $\boldsymbol{q}_d$ which satisfies

$$\lambda_{min}(\boldsymbol{G}(j\omega, \boldsymbol{q}_d) + \boldsymbol{G}^T(-j\omega, \boldsymbol{q}_d)) = 0, \forall\omega \in \Re \qquad (21)$$

is the RAC for total modes where $\lambda_{min}(\boldsymbol{G})$ denotes the minimum eigenvalue of $\boldsymbol{G}$. For this configuration, the condition 1 and 2 of the theorem are satisfied.

C. Stability in the Neighborhood of Robust Arm Configuration for Task-space feedback Control

It is well known that the global stability of task-space control is guaranteed for rigid manipulators[2]. The results obtained in the subsection A suggest that this global stability can not be expected for flexible-base-mounted manipulators with task-space control, since even the linearized mechanism is not positive real over a wide working range. However, it implies that a local asymptotic stability of the original nonlinear system can be guaranteed with a finite but high feedback gain within a small area including the robust arm configuration. The proof is straightforward from Lyapunov indirect method and the passivity theory.

As a result, a high positioning performance can be obtained without considering the base flexibility, i.e, without any additional sensor or solution of a whole inverse dynamics.

D. RAC measure

A robustness measure of arm configuration based on residue matrix has been proposed. It indicates the distance of the existing configuration from the robust arm configuration. Recall that if the rank$(\boldsymbol{R}_i + \boldsymbol{R}_i^T) \leq 2$, there exist only minimum and maximum eigenvalue. $\boldsymbol{G}_i(s)$ is positive real if rank$(\boldsymbol{R}_i + \boldsymbol{R}_i^T) = 1$ and $\lambda_{min}(\boldsymbol{R}_i + \boldsymbol{R}_i^T) \geq 0$ (in fact, this value is negative semi-definite as will be shown below). We has proposed the following robustness measure:

$$w_i(\boldsymbol{q}) = \lambda_{min}(\boldsymbol{R}_i + \boldsymbol{R}_i^T) \qquad (22)$$

This measure directly represents the robustness of the closed-loop stability for given configuration of the manipulator based on the passivity. Hereafter, we call this measure the 'RAC measure'.

The characteristic is that $w_i \leq 0$ holds in general and $w_i = 0$ holds only on the RAC for the ith mode. The configuration where w_i is near 0 is preferable from the view point of the robust stability of the closed-loop system. The advantages of the RAC measure are as follows: First, it can be easily calculated by $n \times n$ numerical computation of eigenvalues. Second, it clarifies the optimality of the arm configuration based on the positive realness. Third, it identifies the robustness for individual mode; this clarifies which mode gives the most serious effect upon the stability. Forth, it does not depend on the underlying control law. Recall that the transfer function $\boldsymbol{P}(s, \boldsymbol{q}_d)$ is given by the mechanical system and the Jacobian transpose.

TABLE I
Link Parameters

m_1	20.0(kg)	l_1	0.2(m)
m_2	7.0(kg)	l_2	0.3(m)
m_3	5.0(kg)	l_3	0.25(m)
I_{x1}	0.009(kgm^2)	l_{g1}	0.02(m)
I_{x2}	0.00315(kgm^2)	l_{g2}	0.15(m)
I_{x3}	0.00225(kgm^2)	l_{g3}	0.125(m)
I_{y1}	0.07116(kgm^2)	I_{z1}	0.07116(kgm^2)
I_{y2}	0.0541(kgm^2)	I_{z2}	0.0541(kgm^2)
I_{y3}	0.0272(kgm^2)	I_{z3}	0.0272(kgm^2)

IV. Redundancy Solution based on RAC Measure

In this section, a method of determining the redundant degree of freedom is proposed. As briefly described in Section II, a configuration $\tilde{\boldsymbol{q}}_d$ should be determined to maximize the RAC measure $w_i(\boldsymbol{q}_d)$ from the view point of the closed loop stability. Recall that $w_i(\boldsymbol{q}_d) \leq 0, ^\forall i$, therefore the configuration is the RAC if $w_i(\tilde{\boldsymbol{q}}_d) = 0$ holds and the ith mode is not destabilized by any end-point control law.

Let $\boldsymbol{\Theta}$ be a set of arm configuration which realizes $\boldsymbol{r}_d$. The optimal arm configuration for $\boldsymbol{r}_d$ considering the ith mode is be given by:

$$\tilde{\boldsymbol{q}}_d = argmax_{\boldsymbol{q}_d \in \boldsymbol{\Theta}} \; w_i(\boldsymbol{q}_d) \qquad (23)$$

where $\boldsymbol{\Theta} = \{\boldsymbol{q}_d | \boldsymbol{r}(\boldsymbol{q}_d) = \boldsymbol{r}_d\}$.

It depends on the number of the redundant DOF $(n - 3)$ and the modes m how many modes can be taken into consideration. For example, in case of $m > n-3$, all modes cannot be stabilized and a determination based on certain priority is necessary[18]. In general, the priority of modes with lower natural frequencies should be set higher[19].

V. Simulation

A. Link Parameters and Control law

Table I shows the link parameters of the manipulator shown in Fig. 1. θ_i is the joint angle of axis i, m_i is the mass , l_i is the length, and l_{gi} is the distance between the axis i and the center of mass of link i. I_{xi}, I_{yi}, and I_{zi} are the moment of inertia around each axis of link i. The base flexibility is approximated as a visco-elastic joint with the stiffness and viscous constants given by $k_{p1} = 3.0 \times 10^4$(Nm/rad),$k_{v1} = 2.0$(Nms/rad). We assume that no singular configuration is passed while working.

The applied controller is a task-space PD feedback controller using Jacobian transpose without considering the base flexibility: $\boldsymbol{K}_c(s) = \boldsymbol{K}_p + \boldsymbol{K}_v s$, then the actuator torque is calculated as:

$$\boldsymbol{\tau}_a = -\boldsymbol{J}_v^T(\boldsymbol{q}_a)(\boldsymbol{K}_p \boldsymbol{y} + \boldsymbol{K}_v \dot{\boldsymbol{y}}) + \boldsymbol{g}(\boldsymbol{q}_a) \tag{24}$$

where $\boldsymbol{K}_p = \mathrm{diag}(8.0 \times 10^4, 8.0 \times 10^4, 8.0 \times 10^4)$(N/m), $\boldsymbol{K}_v = \mathrm{diag}(2.4 \times 10^3, 2.4 \times 10^3, 2.4 \times 10^3)$(Ns/m) respectively. The Coriolis compensation can be added for marginally improving the positioning performance, but this second-order term is not related to the closed loop stability. The control structure and its gains are fixed to make clear the fundamental control performance for a specific arm configuration. Recall the calculation of the RAC measure does not include this PD feedback control, therefore, the determination of the redundancy is not dependent on the underlying controller.

B. Redundancy Determination based on the RAC measure

The optimal configuration for desired tip position $\boldsymbol{r}_d = [0.2, 0.4, -0.2]$ is determined. Due to 1 DOF redundancy, we use θ_4 as a parameter which is directly related with the arm angle. The RAC measure is calculated for $0 \le \theta_4 \le 2\pi$ and remaining joint angle is determined to realize $\boldsymbol{r}_d$. Fig. 3 shows the calculated RAC measure. The natural frequency of the vibration mode is dependent on the arm configuration, which is shown in Fig. 4. By changing θ_4, the elbow trajectory draws a circle, as shown in Fig. 5.

From Fig. 3, the most robust arm configuration is given by $\theta_4 = 3.58$(rad). Since the measure equals to the upper limit zero, this configuration is the RAC. On the contrary, the worst robust configuration is given by $\theta_4 = 6.22$(rad).

A task-space feedback control is applied for the obtained optimal case and the worst case. Fig. 6 and Fig. 7 show the positioning error of the tip for both cases when the tip is released from the neighborhood of the desired position. As shown in Fig. 6, the error converges satisfactorily for the optimal case. Contrary, as shown in Fig. 7, the error diverges and the system becomes unstable on the worst case. However, as shown in Fig. 4, the natural frequencies of the optimal and the worst case are almost the same. Therefore, it can be considered that this difference of the stability mainly comes from the difference of the arm dynamics.

Next, the optimal configuration is determined by the same method for each tip position set on the segment from $[0.2, 0.1, -0.1]$ to $[0.2, 0.3, -0.4]$. We set 10 desired points $\boldsymbol{r}_{di}$ with constant interval as $\boldsymbol{r}_{d1} = [0.2, 0.1, -0.1]$, $\cdots$, $\boldsymbol{r}_{d10} = [0.2, 0.3, -0.4]$. Fig. 8 shows the tip positions and obtained configurations. Fig. 9 shows the RAC measure for each tip position.

In the range of $\boldsymbol{r}_{d1}$ to $\boldsymbol{r}_{d7}$, where the tip is near the body and approximately $\theta_5 < \pi/2$, the configuration in which the elbow joint is jutted out of the shoulder gives high robustness. On the contrary, in the range of $\boldsymbol{r}_{d8}$ to $\boldsymbol{r}_{d10}$ where approximately $\theta_5 > \pi/2$, the configuration in which the elbow joint is inside from the shoulder gives high robustness. As shown in Fig. 9, there is two peaks of robustness, i.e., $0 < \theta_4 < 0.5\pi$ and $\pi < \theta_4 < 1.5\pi$. The highest point is changed between $\boldsymbol{r}_{d7}$ and $\boldsymbol{r}_{d8}$. Although the RAC does not exist for all tip positions, if a configuration is determined based on the RAC measure, the dynamics becomes more close to passive, which leads to the improvement of robustness. However, considering the joint angle limitations, neither human nor a humanoid takes the optimal configuration obtained for $\boldsymbol{r}_{d8}$ to $\boldsymbol{r}_{d10}$. Therefore, when the joint angle is limited like human, it is desirable to do precise task in the range of approximately $\theta_5 < \pi/2$, or choose the second best configuration.

VI. Conclusion

In this paper, a method of redundancy solution for a human-like manipulator mounted on flexible body has been proposed where the base flexibility caused not only by the structure but also by servo control of the body. By this method, the arm configuration is optimized based on the RAC-measure for a task-space feedback control. A high positioning performance can be obtained without considering the base flexibility. The validity has been confirmed by a numerical example performed with a 4 DOF human-like redundant manipulator mounted on a 1 DOF flexible base. A high-bandwidth control has been realized by a task-space controller without considering the base flexibility. The fu-

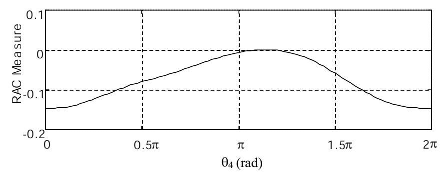

Fig. 3. RAC measure versus θ_4

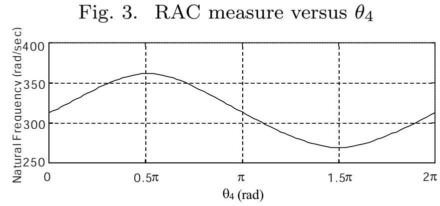

Fig. 4. Natural Frequency versus θ_4

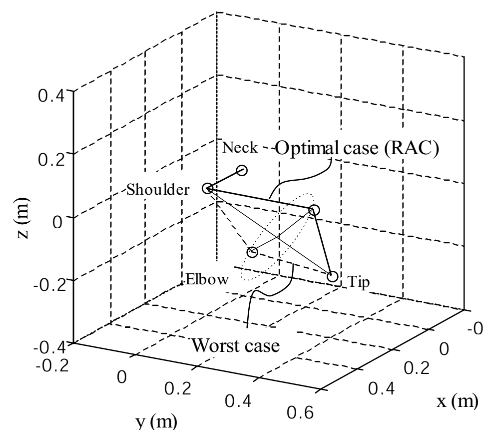

Fig. 5. Optimal and Worst Arm Configuration

ture work includes an expansion to a multiple DOF flexible body and an experiment on a humanoid hardware.

References

[1] M. A. Toress, S. Durowsky, "Path-planning in elastically constrained space manipulator systems", *Proc. IEEE Int. Conf. Robotics and Automation*, pp.812–817, 1993.

[2] S. Arimoto, F. Miyazaki, "Asymptotic Stability of Feedback Laws for Robot Manipulators", *Proc. 1st IFAC Symposium of Robot Control*, pp. 447–452, 1985.

[3] R. H. Cannon, E. Schmitz, "Initial Experiments on the End-Point Control of a Flexible One-Link Robot", *Int. J. Robotics Research*, Vol. 3, No. 3, pp. 62–74, 1984.

[4] M. W. Spong, "Modeling and Control of Elastic Joint Robots", *ASME J. Dynamic Systems, Measurement and Control*, Vol. 109, pp.310–319, December, 1987.

[5] P. Tomei, "A Simple PD Controller for Robots with Elastic Joints", *IEEE Trans. Automatic Control*, Vol. 36, No. 10, pp.1208–1213, October, 1985.

[6] K. Osuka, F. Matsuno, "On Robustness of passivity of manipulators", *Proc. IEEE Conf. Decision and Control*, pp. 3406–3409, 1999.

[7] A. De Luca, "Feedforward/Feedback Laws for the Control of Flexible Robots", *Proc. IEEE Int. Conf. Robotics Automat.*, pp.233–240, 2000.

[8] D. N. Nenchev, K. Yoshida, P. Vichitkulsawat, M. Uchiyama, "Reaction Null-Space Control of Flexible Structure Mounted Manipulator Systems", *IEEE Trans. Robotics Automat.*, Vol. 15, No. 6, 1999.

[9] Z. H. Jiang, "Dynamic Manipulation Characteristics of Robot Arms Mounted on a Flexible Space Structure", *Automatic Control in Aerospace, Proc. of 14th IFAC Symposium.*, 1998.

[10] A. Konno, M. Uchiyama, Y. Kito, M. Murakami, "Configuration-Dependent Vibration Controllability of Flexible-Link Manipulators", *Int. J. Robotics Research*, Vol. 16, No. 4, pp. 567 - 576, 1997.

[11] T. Yoshikawa, "Dynamic Manipulability of Robotic Mechanism", *J. Robotic Systems*, Vol. 2 No. 1, pp.113–124, 1985.

[12] J. Ueda, T. Yoshikawa, "Robust Arm Configuration of Manipulator Mounted on Flexible Base", *Proc. IEEE Int. Conf. Robotics and Automation*, pp.1321-1326, 2002.

[13] Jun Ueda, Tsuneo Yoshikawa, "Mode Shape Compensator for Improving Robustness of Manipulator Mounted on Flexible Base", *IEEE Trans. Robotics and Automation, accepted.*

[14] T. Iwasaki, "Integrated System Design by Separation", *Proc. IEEE Conf. Control Application*, pp.97–102, August, 1999.

[15] K. Kreutz-Delgado, M. Long, H. Seraji, "Kinematic Analysis of 7-DOF Manipulators", *Int. J. Robotics Research*, Vol. 11, No. 5, pp. 469–481, 1992.

[16] C. T. Chen, C. A. Desser, "Controllability and Observability of Composite Systems", *IEEE Trans. Automatic Control*, Vol. 12, No. 4, pp.402–409, August, 1967.

[17] B. D. O. Anderson, S. Vongpanitlerd, "Network Analysis and Synthesis", Prentice-Hall, 1973.

[18] J. Ueda, "Design and Control of Stable and High-performance Mechatronic Systems", Ph.D Thesis, Kyoto University, 2002.

[19] T. Yoshikawa, J. Ueda, "Task Priority Based Mode Shaping Method for In-phase Design of Flexible Structures Aiming at High Speed and Accurate Positioning", *Proc. IEEE Int. Conf. Robotics and Automation*, pp.1806–1812, 2001.

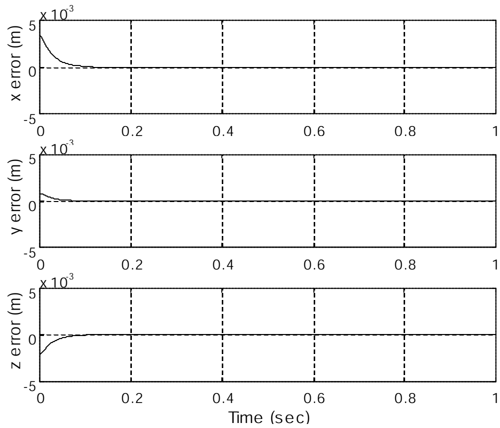

Fig. 6. Positioning Error with Optimal Configuration

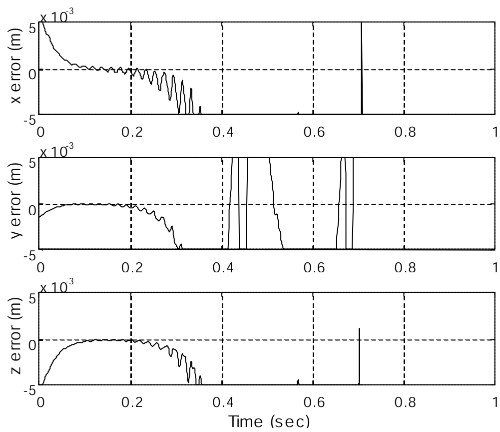

Fig. 7. Positioning Error with Worst Configuration

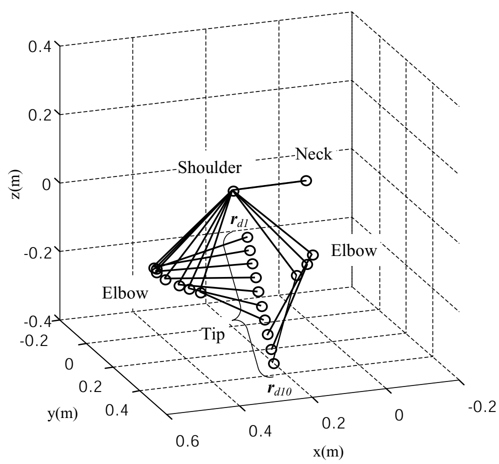

Fig. 8. Optimal Configuration

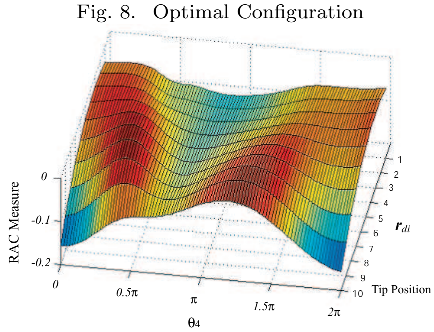

Fig. 9. RAC Measure